



# New dual-mode orthogonal tunable fluorescence systems based on cucurbit [8]uril: White light, 3D printing, and anti-counterfeit applications

Ting Ting Zhang<sup>a</sup>, Xi Nan Yang<sup>a</sup>, Jian Hang Hu<sup>a</sup>, Yang Luo<sup>a</sup>, Hou Jing Liu<sup>a</sup>, Zhu Tao<sup>a</sup>, Xin Xiao<sup>a,\*</sup>, Carl Redshaw<sup>b,\*</sup>

<sup>a</sup> State Key Laboratory Breeding Base of Green Pesticide and Agricultural Bioengineering, Key Laboratory of Green Pesticide and Agricultural Bioengineering, Key Laboratory of Macrocyclic and Supramolecular Chemistry of Guizhou Province, Guizhou University, Guiyang 550025, China

<sup>b</sup> Department of Chemistry, University of Hull, Hull HU6 7RX, UK

## ARTICLE INFO

### Keywords:

Supramolecular approach  
Perylene  
White light emission  
Host-guest interaction  
Cucurbit[n]urils

## ABSTRACT

In this work, we have utilized a supramolecular approach to control emission, and generate white light and have applied the system to both 3D printing and counterfeiting applications. In particular, we report two new dual-mode orthogonal tunable fluorescence systems, A and B. System A is based on the fluorescent dyes perylene diimide (PDI-C6) and 7-hydroxycoumarin, which are incorporated into the main guest system, namely cucurbit [8]uril (Q[8]). This system can provide bright white emission and proved to be adaptable, whereby the emission can be easily changed via temperature control; a smart temperature control switch in the range of 30 °C to 100 °C was developed. System B is based on quinine sulfate with PDI-C6 and Q[8], and this system can provide white emission over a wide concentration range and it was applied to LED lamps. Such white emission also performs well in polymeric matrices and can be utilized for 3D printing, whilst solutions can be used for more practical applications, for example as anti-counterfeiting materials.

## 1. Introduction

The host-guest chemistry of cucurbit[n]urils, Q[n]s, is currently a hot topic in supramolecular chemistry, particularly given their ability to bind cationic organic species in an aqueous solution [1,2]. Moreover, systems that combine cucurbiturils with fluorescent dye guests and enable such systems to act as fluorescent switches or sensors are of great interest [3–6]. In this area, Scherman *et al.* (with Q[8]) [7], Zhang *et al.* (with Q[7]) [8], Hunter and Huang *et al.* (with Q[8]) [9], have reported significant host-guest systems that involve naphthalene-containing perylene diimide (PDI) as the rigid core of the guest with applications involving free radical production and sensors. Meanwhile, Xu, Zhang, and coworkers have recently employed a Q[7]@PDI system in photo-thermal therapy [10], whilst Yang and An have employed a Q[7]/PDI containing system to enhance the rate of catalysis during the RAFT photo-polymerization of *N,N'*-dimethylacrylamide [11]. The interest in PDI stems from its inherent desirable properties that include electron-accepting ability, enhanced thermal and optical properties, high extinction coefficients, and excellent quantum yields [12–19]. In water, the planar conjugated structure tends to promote  $\pi$ - $\pi$  stacking and a lack

of fluorescence. The presence of the Q[n] aids the depolymerization process and allows for the formation of fluorescent supramolecular systems [6,13–23]. By varying other parameters such as pH, the emission can be controlled, for example, to produce white light [24–30]. The presence of other guests can also impact the behavior of the system. There is thus a need to further develop combinations of guests and Q[n]s to expand the armory of available and tunable supramolecular emissive systems. The dynamic behavior of these systems though is challenging, but if control of individual complementary colors can be achieved, then this would be of technological relevance to, for example, OLED technology [5,31–39]. Other notable approaches to dual-mode fluorescence modulation of supramolecular systems include locking/unlocking of vibrational emissive units [40], and regulation of  $\pi$ -conjugated wings in dihydrophenazine-type systems [41].

PDI molecules have many good attributes including their good stability, high coloration, photostable, strong  $\pi$ - $\pi$  conjugation effects, an electron affinity energy comparable to that of fullerenes, strong electron deficiency properties, tunable solubility, and excellent photoelectric properties [42–44]. However, PDI molecules tend to form non-fluorescent  $\pi$ - $\pi$  stacks in water, which hampers their function in

\* Corresponding authors.

E-mail addresses: [gyhxxiaoxin@163.com](mailto:gyhxxiaoxin@163.com) (X. Xiao), [c.redshaw@hull.ac.uk](mailto:c.redshaw@hull.ac.uk) (C. Redshaw).

<https://doi.org/10.1016/j.cej.2022.138960>

Received 6 June 2022; Received in revised form 27 August 2022; Accepted 29 August 2022

Available online 13 September 2022

1385-8947/© 2022 The Author(s). Published by Elsevier B.V. This is an open access article under the CC BY license (<http://creativecommons.org/licenses/by/4.0/>).

aqueous systems, and greatly limits the application of PDIs as photo-voltaic materials [45–49]. The adoption of a supramolecular approach not only alleviates the negative effects of PDI-C6 intermolecular interactions and energy transfer processes but also confers color tunability and stimulus responsiveness to the white light-emitting materials due to the dynamic and reversible nature of the non-covalent interactions present. Indeed, well-structured supramolecular materials can regulate energy transfer through an assembly-disassembly process and can lead to potentially diverse applications. In general, supramolecular chemistry focuses on chemical systems consisting of assembled molecular subunits or components. Unlike traditional chemistry based on covalent interactions, it utilizes weak and reversible non-covalent interactions, including hydrogen bonding, metal coordination, hydrophobic forces, van der Waals forces,  $\pi$ - $\pi$  stacking, and electrostatic effects. With such interactions in mind, the supramolecular platform can overcome the problems caused by partial energy transfer from the donor to the acceptor, which therefore provides a new perspective for the construction of tunable luminescent materials. Such supramolecular system tunable white light is widely used in biomedicine, anti-counterfeiting, sensors, and organic light-emitting diodes, but also enables enhanced performance leading to superior fluorescent lamps, thereby providing practical applications for new white light emission. The supramolecular system-controlled fluorescence-tuned emitted white light is regulated by the assembly-disassembly process of energy transfer, and overcomes the problems associated with partial energy transfer from donor to acceptor, making its application greener and simpler. Given these advantages, the supramolecular system-controlled photoluminescence properties and the development of smart color-tunable luminescent materials and their devices have great potential for future applications [49–54].

In this work, we have investigated the construction of two new dual-mode orthogonal tunable fluorescence systems. The first, A, comprises (PDI-C6@Q[8]@7-hydroxycoumarin), whilst the second, B, is (PDI-C6@Q[8]@QSD); PDI-C6 was prepared from *N,N*-bis[diethylamino]-3,4,9,10-perylene tetracarboxylic diimide and 6-bromohexanoic acid (see Fig. S1 in the supplementary section). Within the one system, a series of dye systems with dual fluorescence emission is obtained due to the two simultaneously generated excited states. Excitation at the appropriate wavelength leads to balanced emission from a single excited state, resulting in pure white light emission [37]. Although the preparation of single molecules with white light emission is extremely challenging, by varying the excitation wavelength, the fluorescence intensity associated with 7-hydroxycoumarin/quinine sulfate can be controlled in the supramolecular system and is not affected by Q[8]. In contrast, the emission of PDI-C6 is influenced by Q[8] due to host inhibition of aggregation. In other words, in systems A and B, 7-hydroxycoumarin and quinine sulfate can control the white light emission by using different stimuli, e.g. excitation wavelength, and temperature. Moreover, by using this dual-mode modulation, the system has the potential to cover the entire white light region. It is worth noting here that for the system developed by Qu *et al.*, the application is somewhat limited by the fact that the interaction site between Q[8] and the PDI derivative is on the aromatic ring molecule [13,34]. Here, the use of PDI derivatives with highly water-soluble carboxyl chain arms at the amine site allows for the formation of a 1:2 host-guest fluorescent system (by encapsulation of the chain arms). In addition, the addition of 7-hydroxycoumarin, which exhibits  $\pi$ - $\pi$  conjugation with the aromatic part of PDI-C6, allows for the adjustment of the white light by varying the amounts of Q[8] or PDI in the system. Thus, a new type of temperature control switch has been developed due to its increased solubility and the variable concentration/ratio of the system. We note that the design of water-soluble luminescent materials is more challenging due to their inherent properties. This is because the intrinsic hydrophobic effect of organic chromophores may affect the dispersion and aggregation-induced quenching (ACQ) phenomena. It is also noteworthy here that the use of quinine sulfate can adjust the white light over a wider concentration range, which can be utilized for LED white luminescence. Meanwhile, due to the large

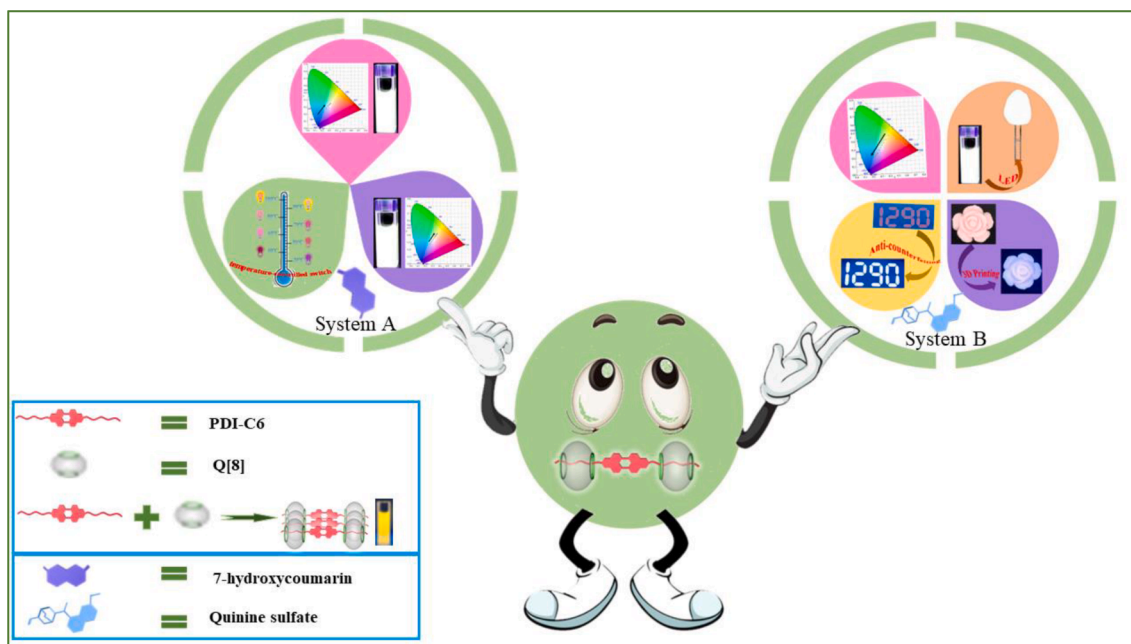
difference in solution color observed under natural light and at 365 nm, the PDI-C6@Q[8]@QSD solution was cast into a polymer material, and EP transparent films were successfully prepared, which showed excellent white luminescence properties. Such hybrid films can be coated onto banknotes for anti-counterfeiting applications, thereby enriching the potential applications of this orthogonal system. The system and components used here are shown in Scheme 1.

## 2. Results and discussion

### 2.1. Supramolecular approach to construct a dual-mode orthogonal white light system

White light systems typically consist of three types of fluorophores and with RGB (red, green, and blue) primary colors mixed simultaneously. White light can be obtained at a single wavelength through an intermolecular energy transfer process, but its rigid action ratio restricts greatly the potential practical applications of white light. In recent years, the use of fluorescence-tuned white light in the orthogonal mode has stimulated interest as a new way of modulating white light. Specifically, in an emission mixing system, the emission intensity of two independent units of complementary fluorescent colors can be tuned by two discrete control units without interfering with each other. For example, blue and yellow can be modulated in the orthogonal mode, resulting in a mixed color emission. In this experiment, two blue fluorescent substances, namely 7-hydroxycoumarin and quinine sulfate, were selected to be added to the PDI-C6@Q[8] supramolecular system, respectively. The fluorescence intensity of 7-hydroxycoumarin and quinine sulfate can be adjusted by the use of different wavelengths of excitation light; the results are given in Fig. 1. For 7-hydroxycoumarin and quinine sulfate, when the excitation wavelength was changed from 320 nm to 380 nm, the fluorescence intensity of these two substances decreased to less than 3 % of the original values, showing a very sensitive change to the applied excitation wavelength. When the excitation wavelength of PDI-C6 was changed from 320 nm to 380 nm, the fluorescence intensity at 375 nm increased to only 2.3 times the fluorescence intensity at 320 nm, showing an insensitive change in the excitation wavelength of PDI-C6. Significant differences in the fluorescence response of the two dyes to changes in excitation wavelength were investigated, which showed that the changing excitation wavelength (blue fluorescence) was response specific for the fluorescence intensity of 7-hydroxycoumarin/quinine sulfate rather than for PDI-C6, *i.e.* the condition of fluorescence modulation of white light in the orthogonal mode was satisfied. Since the fluorescence intensity of 7-hydroxycoumarin can be significantly tuned on changing the excitation wavelength, attention focused on the tuning of PDI-C6. The experimental section provides the synthetic procedure used to prepare fluorescent PDI-C6. The structures of these compounds were confirmed by  $^1\text{H}$  NMR spectroscopy (see Supplementary Information, Fig. S2), and the fluorescence intensity of 7-hydroxycoumarin in system A and quinine sulfate in system B could be tuned significantly on changing the excitation wavelength, thus, as mentioned above, attention focused on tuning PDI-C6.

Given the chemical structure of PDI-C6,  $\pi$ - $\pi$  stacking aggregation is facile in solution, and when Q[8] is added to PDI-C6, a host-guest complex is formed that inhibits this aggregation. This ability to inhibit  $\pi$ - $\pi$  stacking/aggregation greatly increases the fluorescence intensity. Such a host-guest encapsulation strategy provides a more direct way to protect the PDI dye from self-aggregation than arduous synthetic modifications to the dye. Importantly, this approach also provides the opportunity to reversibly switch the fluorescence response by additional chemical stimulation. To further understand the effect of varying the molecular ratio between Q[8] and PDI-C6, several fluorescence and UV spectroscopic experiments were performed. As shown in Fig. 2, PDI-C6 ( $2 \times 10^{-5}$  mol/L) exhibited yellow fluorescence in an aqueous solution, which increased significantly on gradual addition of Q[8] until the



Scheme 1. System A and System B components used herein.

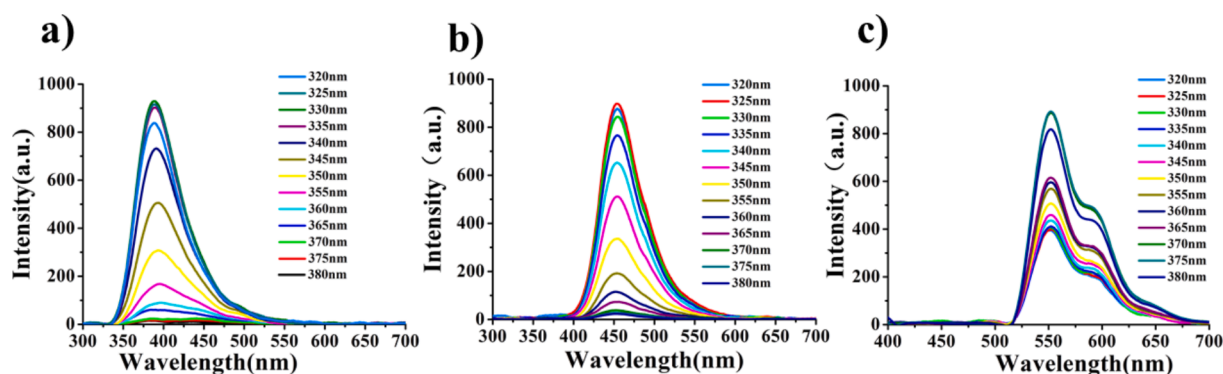


Fig. 1. a) Fluorescence emission spectra of QSD (10  $\mu\text{M}$ ) solution at different excitation wavelengths; b) Fluorescence emission spectra of 7-hydroxycoumarin (10  $\mu\text{M}$ ) solution at different excitation wavelengths; c) Fluorescence emission spectra of PDI-C6 (10  $\mu\text{M}$ ) solutions at different excitation wavelengths.

ratio (of Q[8]@PDI-C6) reached 1:2 (Fig. 2a). This result is consistent with the formation of the supramolecular complex PDI-C6@Q[8], which was further verified by a Job's plot (Fig. S7), with the maximum peak occurring at a molar fraction of 0.33, which corresponds to a Q[8]-PDI-C6 complexation ratio of 1:2 (involving aromatic ring binding of Q[8] to PDI-C6). Isothermal Titration Calorimetry is also consistent with this conclusion (Supplementary Fig. S3). The correlation between the Q[8] concentration and the photophysical properties of the two dyes was then investigated. Titration experiments were carried out by adding Q[8] to the dye solutions. PDI-C6 showed a significant response to the addition of Q[8]. As shown in Fig. 2b, the absorption peak of PDI-C6 at 535 nm increased, while the absorption peak at 500 nm decreased slightly due to the inhibition of Q[8] resulting in a decrease of H-aggregates. No significant changes were observed on addition of 2 equivalents of Q[8], indicating a 1:2 type of host-guest system. Notably, the addition of Q[8] resulted in a significant increase in the fluorescence peak associated with PDI-C6.

In some cases, the encapsulation of the dye leads to profound changes in emission wavelength and quantum yield, as well as an increase in photostability. Since Q[8] has a large cavity, it can simultaneously bind two planar aromatic molecules. For 7-hydroxycoumarin, we propose here a hypothesis based on the special perylene-core of PDI-

C6. 7-Hydroxycoumarin can bind to the perylene nucleus of PDI-C6 through non-covalent interactions to achieve a dynamic equilibrium. On the other hand, the side chain of PDI-C6 enters the cavity of Q[8] for binding. Thus, different fluorescence responses are observed when 7-hydroxycoumarin and PDI-C6 are added to the Q[8] solution alone and when the two guest molecules are added together to the Q[8] solution. This is the key to construct an orthogonal switchable system. For quinine sulfate, we found that quinine sulfate alone can enter the cavity of Q[8] for binding and that the fluorescence intensity of quinine sulfate is changed when it is bound in Q[8]. Given that Q[8] has a large cavity, both the side chain of PDI-C6 and the alkyl portion of quinine sulfate can bind to the Q[8] cavity and achieve dynamic equilibrium, resulting in white light emission.

We first investigated separately whether 7-hydroxycoumarin and quinine sulfate interacted with Q[8]. According to the  $^1\text{H}$  NMR spectra (see Supplementary Information, Fig. S4), no significant changes were found for the proton peaks of 7-hydroxycoumarin after the addition of Q[8] to the 7-hydroxycoumarin solution. Furthermore, 7-hydroxycoumarin showed no response to the addition of Q[8] in the absorption or fluorescence spectra. This is due to the lack of host-guest binding between the neutral 7-hydroxycoumarin and the Q[8]. To further confirm the orthogonality, titration experiments were performed in which 7-

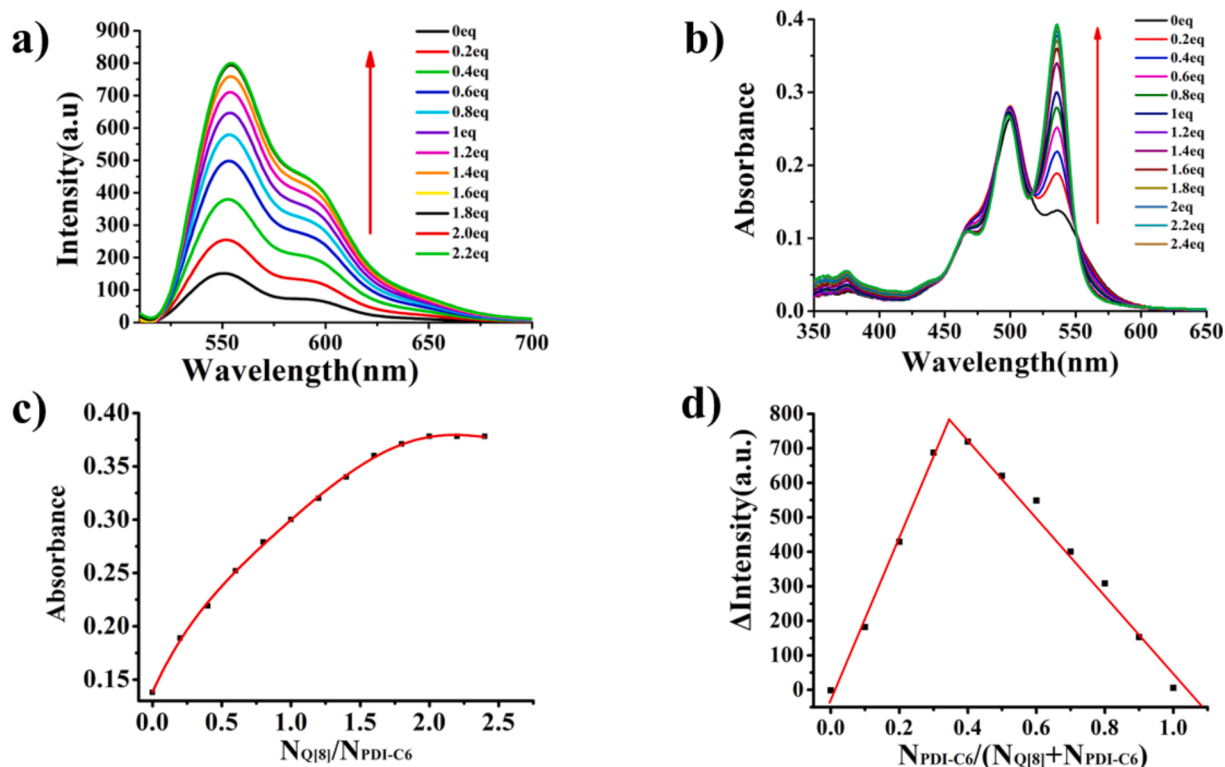


Fig. 2. a) Fluorescence emission (upon excitation at 375 nm); b) UV-vis absorption spectra of PDI-C6 (20 μM) solution with increasing concentrations of Q[8].

hydroxycoumarin was added to aqueous solutions of PDI-C6 and Q[8] in a 1:2 M ratio (see [Supplementary Information, Fig. S8c, d](#)). The absorption and fluorescence spectra showed no significant change for the peak of PDI-C6@Q[8] when the concentration of coumarin was increased. Thus, the two dyes 7-hydroxycoumarin and PDI-C6 exhibit different fluorescence responses when Q[8] is added, which is essential for the construction of an orthogonal switchable system. Next, we investigated whether there was a non-covalent interaction between PDI-C6 and 7-hydroxycoumarin. The proton peaks Hn, Ho, Hp, Hq, and Hm of 7-hydroxycoumarin moved to a higher field, and the proton peaks of the PDI-C6 alkyl chain also moved to higher field (see [Supplementary Information, Fig. S5](#)). However, the two proton peaks of the benzene ring of PDI-C6, Hi and Hj, moved to lower field. In addition, Hi on PDI-C6 was found to move to the same position as the Ho peak of 7-hydroxycoumarin, while Hj on PDI-C6 moved to the same position as the Hn peak of 7-hydroxycoumarin. These phenomena indicate that there may be noncovalent interactions between PDI-C6 and 7-hydroxycoumarin. For quinine sulfate @ Q[8], it was found that the proton peaks of the quinoline part of quinine sulfate were all shifted to low field, while the proton peaks on the alkyl ring were all shifted to high field, indicating that the alkyl part of quinine sulfate entered the Q[8] cavity for binding, while the quinoline part was outside the Q[8] cavity (see [Supplementary Information, Fig. S9](#)). Also, when the Q[8] is not yet present, the peaks of quinine sulfate are not shifted, which indicates that the mode of action of system B is different from that of the system A. As shown in the fluorogram, the peak fluorescence intensity of quinine sulfate at 375 nm decreased and was red-shifted (and enhanced) to 475 nm when 10 μM of quinine sulfate solution was added to Q[8] (see [Supplementary Information, Fig. S11](#)). This confirms our proposed different modes and mechanisms of action for the two tuned white light systems.

For an ideal organic light-emitting material (and device), the two complementary colors should be tuned in an orthogonal mode, which means that in an emission mixing system, the blue and yellow emission intensities are in dynamic equilibrium, and the supramolecular control unit is tuned without interference. The fluorescence emission of 7-

hydroxycoumarin can be easily tuned by the excitation wavelength ([Fig. 1b](#)), while the fluorescence emission of PDI-C6 remains unchanged. Given its inherent special properties, for the mixture of 7-hydroxycoumarin and PDI-C6 added to Q[8] solution, as shown in the fluorescence spectrum in [Fig. S10](#), the fluorescence intensity of the characteristic peak of PDI-C6 at 550 nm gradually increased, and when 0.2 times Q[8] was added, its fluorescence intensity was the same as that of the characteristic peak of 7-hydroxycoumarin at 450 nm, and the solution exhibited white fluorescence under such conditions. Unlike the mode of action of 7-hydroxycoumarin, the alkyl portion of the quinine sulfate can enter the cavity of the Q[8] as shown in [Fig. S11](#). The fluorescence spectrum was red-shifted by a difference of 100 nm when quinine sulfate was added to Q[8] and the fluorescence intensity was enhanced, thus tuning the white light differently when 7-hydroxycoumarin was employed. When quinine sulfate was added to the system of PDI-C6@Q[8] (10 μM; 1:2), the peak of quinine sulfate at 466 nm was blue-shifted, and when quinine sulfate was added to the system of PDI-C6@Q[8] (10 μM; 1:2), the peak of PDI-C6 decreased in fluorescence intensity at 555 nm, when the presence of quinine sulfate reached 1.0 equiv. i.e., the fluorescence intensity reaches equilibrium. This indicates that quinine sulfate and PDI reach equilibrium in the cavity of the Q[8] in a 1:1 ratio (see [Supplementary Information, Fig. S12](#)).

## 2.2. Construction of white light LEDs

Based on the above results, after confirming that the two supramolecular fluorescence systems can be bimodally orthogonally tuned, we measured the fluorescence spectra of the two systems in an orthogonal manner (by adding Q[8] solution or PDI-C6 solution and using different excitation wavelengths). We found that for system A, following the addition of Q[8] to the solution of PDI-C6 (10 μM) @ 7-hydroxycoumarin (10 μM), by varying the excitation wavelength modulated the blue-yellow light, there was an increase in fluorescence intensity (see [Supplementary Material Fig. S10a, b](#)). As shown in [Fig. 3](#), when 0.2 equivalents of Q[8] were used, white light emission was obtained at 365

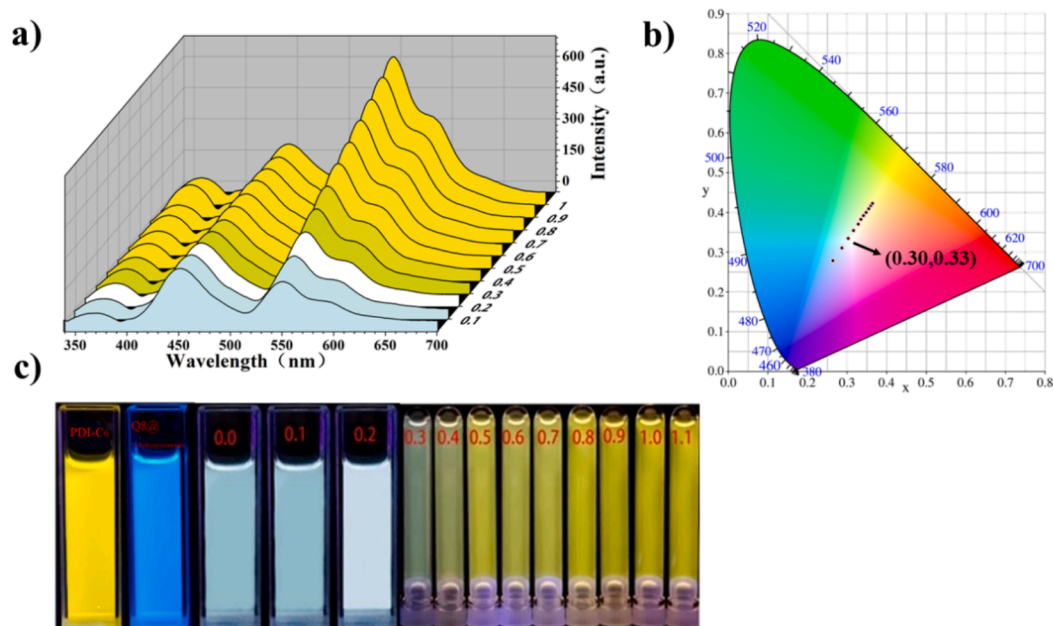


**Fig. 3.** a) Mixed solution (7-hydroxycoumarin, 10  $\mu\text{M}$ ; PDI-C6, 10  $\mu\text{M}$ ) at increasing concentrations of Q[8], b-c) color changes from blue to yellow, and the corresponding CIE coordinate diagram of PDI-C6 (10  $\mu\text{M}$ ) and 7-hydroxycoumarin (10  $\mu\text{M}$ ) solution on increasing concentrations of Q[8].

nm excitation with a CIE (0.30, 0.33) close to that of pure white light (0.33, 0.33). When Q[8] is added continuously, the fluorescence intensity was enhanced. A fluorescence change was observed when employing a 365 nm UV lamp on the system, and it was found that the solution changed from an initial blue color to white and finally to yellow with the addition of Q[8], as shown in Fig. 4. Similarly, the addition of PDI-C6 to a solution of Q[8] (10  $\mu\text{M}$ ) and 7-hydroxycoumarin (10  $\mu\text{M}$ ) also tuned the blue-yellow light (see Supplementary Material, Fig. S10c, d). When 0.3 equiv. of PDI-C6 was added, white emission was obtained at 365 nm; CIE (0.33, 0.29). However, when 0.6 equivalents of PDI-C6 were added, there was almost no change in fluorescence intensity. The fluorescence changes were observed for this system using a 365 nm UV lamp, and it was found that the solution changed from blue to white and

finally to yellow with the addition of PDI-C6.

In addition, for system A: the Q[8] (2  $\mu\text{M}$ )@PDI-C6 (10  $\mu\text{M}$ )@Q7-hydroxycoumarin (10  $\mu\text{M}$ ) system and the PDI-C6 (2  $\mu\text{M}$ )@Q[8] (10  $\mu\text{M}$ )@Q7-hydroxycoumarin (10  $\mu\text{M}$ ) system were excited at 355–370 nm excitation wavelengths, respectively, as shown in Fig. 5a and c. It can be seen that the intensity of the characteristic peak of 7-hydroxycoumarin varies with different emission wavelengths, while the intensity of the characteristic peak of PDI-C6 hardly changes, and for Q[8] (2  $\mu\text{M}$ ) @ PDI-C6 (10  $\mu\text{M}$ ) @ Q7-hydroxycoumarin system (10  $\mu\text{M}$ ) the CIE changes from blue CIE (0.20, 0.19) to yellow (0.39, 0.48) (Fig. 5d). For the PDI-C6 (2  $\mu\text{M}$ ) @ Q[8] (10  $\mu\text{M}$ ) @ Q7-hydroxycoumarin system (10  $\mu\text{M}$ ), the system CIE coordinates changed from (0.21, 0.21) to yellow CIE (0.37, 0.46) (Fig. 5b), which showed that intermolecular energy transfer

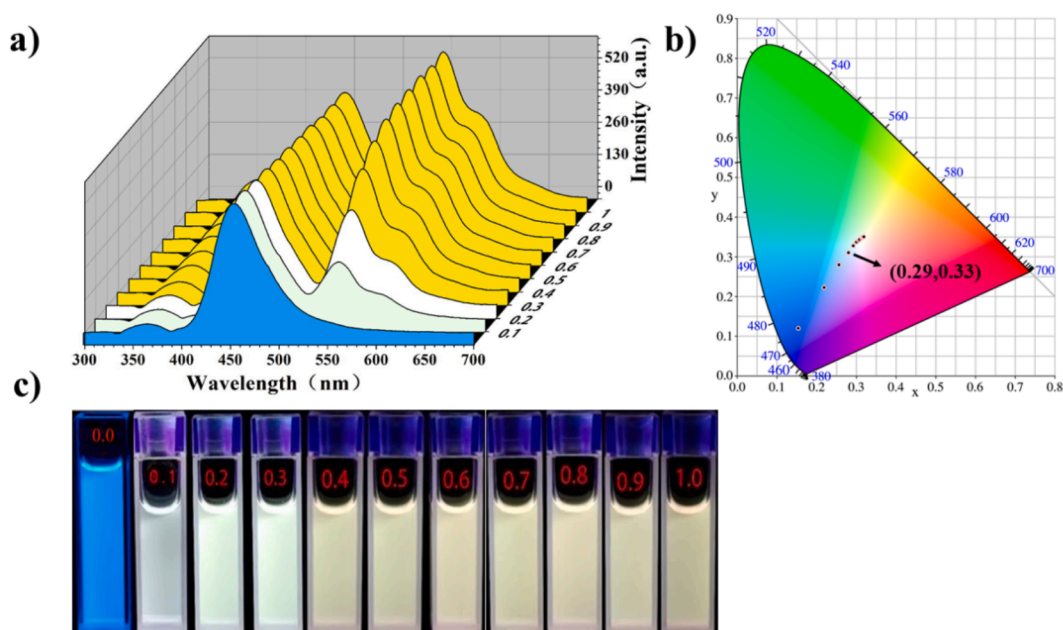


**Fig. 4.** a) Mixed solution (7-hydroxycoumarin, 10  $\mu\text{M}$ ; Q[8], 10  $\mu\text{M}$ ) with increasing concentrations of PDI-C6, b-c) color changes from blue to yellow and corresponding CIE coordinate diagram of (Q[8], 10  $\mu\text{M}$ ) and 7-hydroxycoumarin (10  $\mu\text{M}$ ) solution on increasing concentrations of PDI-C6.

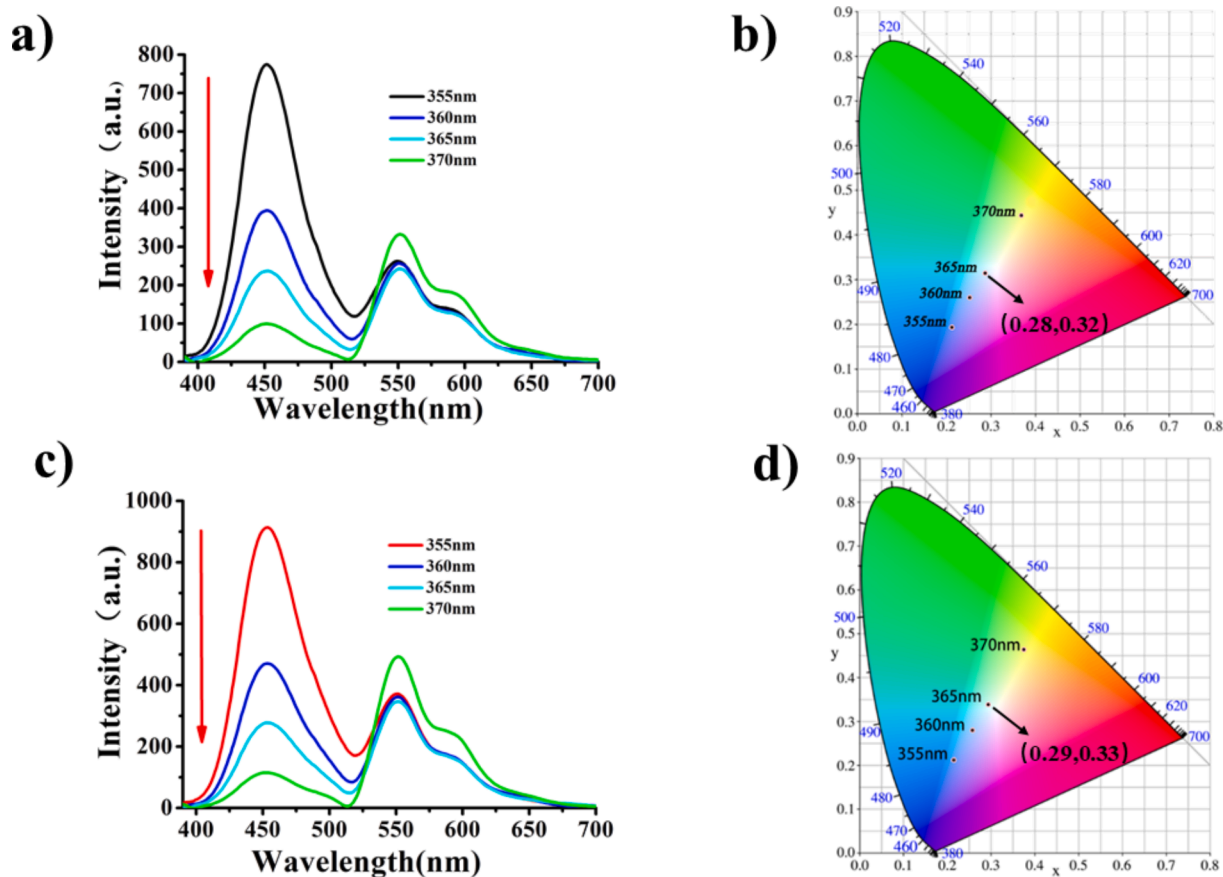


Fig. 5. a) Fluorescence emission spectra of the mixture solution (7-hydroxycoumarin, 10  $\mu\text{M}$ ; Q[8], 2  $\mu\text{M}$ ; PDI-C6, 10  $\mu\text{M}$ ); b) CIE of the mixed solution (7-hydroxycoumarin, 10  $\mu\text{M}$ ; PDI-C6, 10  $\mu\text{M}$ ; Q[8], 2  $\mu\text{M}$ ) at different excitation wavelengths from 350 nm to 370 nm, the color changed from blue to yellow; c) Fluorescence emission spectra of the mixed solution (7-hydroxycoumarin, 10  $\mu\text{M}$ ; Q[8], 10  $\mu\text{M}$ ; PDI-C6, 2  $\mu\text{M}$ ); d) CIE of the mixed solution (7-hydroxycoumarin, 10  $\mu\text{M}$ ; Q[8], 10  $\mu\text{M}$ ; PDI-C6, 2  $\mu\text{M}$ .) at different excitation wavelengths from 350 nm to 370 nm, the color changed from blue to yellow.

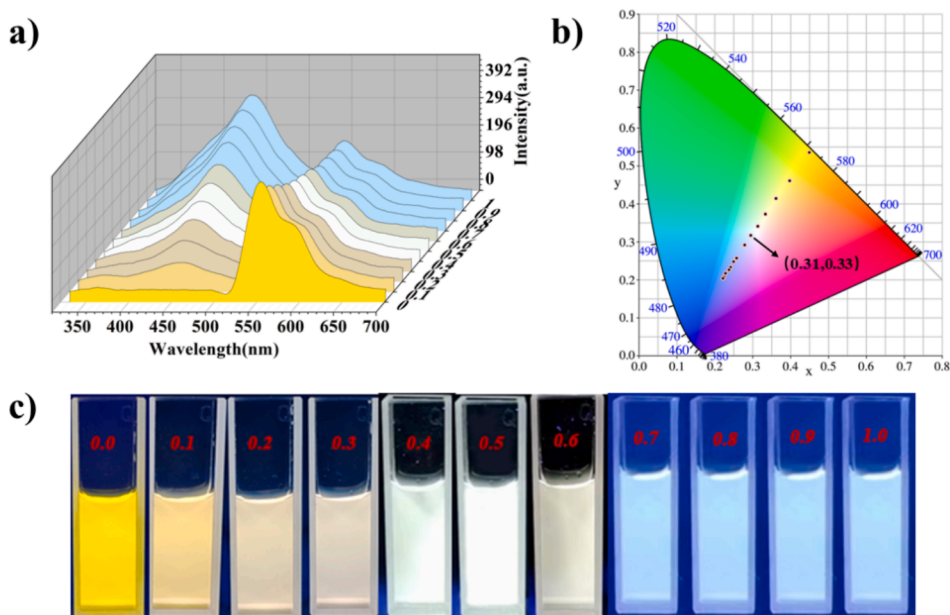


Fig. 6. a) Fluorescence spectra of PDI-C6 (10  $\mu\text{M}$ ); Q[8] (20  $\mu\text{M}$ ) with increasing quinine sulfate concentration; b) CIE coordinates for PDI-C6 (10  $\mu\text{M}$ ); CIE coordinates for Q[8] (20  $\mu\text{M}$ ) at increasing quinine sulfate are (0.31, 0.33) when quinine sulfate is 0.5 equivalents; c) PDI-C6 (10  $\mu\text{M}$ ); Q[8] (20  $\mu\text{M}$ ) at increasing quinine sulfate concentration, the color changes from yellow to white to blue.

can be tuned to white light by changing the excitation wavelength, providing a clear tuning pattern for white light applications.

For system B, the blue-yellow light can be modulated by changing the excitation wavelength and adding quinine sulfate to the solution of PDI-C6 (10  $\mu$ M) @ Q[8] (10  $\mu$ M), see Fig. 6. The fluorescence spectrum shows that the peak of the quinine sulfate at 466 nm is blue-shifted, while for the peak of PDI-C6 at 555 nm, the fluorescence intensity decreases. When the molar amount of quinine sulfate in the system reached 1.0 equivalent to PDI-C6, the intensity of the characteristic peak of quinine sulfate gradually increased with the increase of concentration, while the characteristic peak of PDI-C6 at 550 nm decreased to a constant trend, which shows that the alkyl part of quinine sulfate entered the cavity part of the Q[8], and at the same time, the fluorescence intensity of PDI-C6 decreased. This proved that the quinine sulfate and the PDI-C6 reached equilibrium in the cavity of the Q[8] at a ratio of 1:1. As shown in Fig. 6c and d, with 0.4 equiv. and 0.5 equiv. of quinine sulfate, white light emission was obtained under excitation at 365 nm with CIEs of (0.29, 0.31); (0.31, 0.33) close to the CIE of pure white light (0.33, 0.33), respectively. When quinine sulfate was added continuously, the intensity of the characteristic peak of quinine sulfate was enhanced, while the fluorescence intensity of the characteristic peak of PDI-C6 decreased continuously, and the CIE (0.29, 0.32) showed cold white light when 0.6 equiv. of quinine sulfate was added, and the fluorescence color gradually turned blue until almost no change occurred when 0.7 equivalent was added.

It is clear that for the two supramolecules A and B, when the fluorescence intensity of the blue and yellow molecules in the system are equal, the system reaches a blue-yellow dynamic equilibrium and emits white light in the white region of the CIE diagram. Thus, when quinine sulfate is added to the strong yellow solution of Q[8]@PDI-C6, the fluorescence CIE goes from the yellow to the blue region, and the emission band of quinine sulfate in the presence of PDI-C6@Q[8] covers almost the entire region of the visible spectrum during the whole titration, with a calculated CIE coordinate of (0.31, 0.33), which is close to that of pure white light (0.33, 0.33). In the fluorescence spectrum, when the characteristic peak of quinine sulfate at 450 nm has the same fluorescence intensity as the characteristic peak of PDI-C6@Q[8] at 550 nm, then the system exhibits white light emission. This feature was also demonstrated in the PDI-C6@Q[8]@7-hydroxycoumarin liquid, where the tunable color emission within the white light of both systems came from an equilibrium mixture, showing the potential for tunability. The tunable color emission of both systems, including white light, came from an equilibrium mixture, and the emission of the fluorescence of PDI-C6 was greatly improved by the addition of Q[8] to the mixture under 375 nm excitation, i.e. higher fluorescence quantum yields and fluorescence lifetimes (see Supplementary Fig. S13, S14). Such results show the potential for application of this system in the construction of organic white-light emitting materials with tunable and responsive properties.

The conventional white light system mixes three types of fluorophores (red, yellow, and blue) at the same time and is structured by a multi-component energy transfer process. This strategy requires a strictly fixed ratio and carefully designed energy matching of the three fluorophores, which has a large limitation, while the current A and B systems are obtained by stimulus induction and are controlled by supramolecular bodies with energy resonance tuning. Due to this unique supramolecular structure, its blue and yellow fluorescence can be used to build a white light system emitted by LEDs. Both A and B mentioned above show dual blue fluorescence and yellow emission, which can be tuned by controlling the ratio between each other. Such characteristics make the supramolecular assembly suitable for constructing LEDs with stable fluorescence spectra and CIE coordinates that demonstrate good stability and specificity of white light emission at room temperature.

### 2.3. Construction of a temperature-controlled switch

In this systematic study of PDI-C6@7-hydroxycoumarin@Q[8], we

developed a novel bimodal orthogonal tunable supramolecular fluorescence system. It was found that the fluorescence colors of the system were different at low and high temperatures when the system reached a certain concentration. We hypothesized that the whole system could not only adjust the system color by different ratios but also by adjusting the temperature experienced by the host-guest system, which leads to the observed fluorescence color change. Based on this conjecture, we conducted the following experiments. Firstly, we prepared solutions of PDI-C6 (1 mmol), Q[8] (0.1 mmol), and 7-hydroxycoumarin (5 mmol) and then subjected the solutions to programmed temperature changes from 30 °C to 100 °C and observed the color changes under natural light and 365 nm UV light. The results are shown in Fig. 7a and b. The solution changed from an initial purple-red color to red and finally to a yellow solution. These actions here caused by the temperature may occur for several reasons: (i) High temperatures may disrupt non-covalent interactions or result in dynamic equilibrium exchange more frequently; (ii) Decrease in the emission intensity due to increased non-radiative conversion; (iii) may contribute to solubility by reducing any form of aggregation. Thus, as the temperature increases, the noncovalent interactions in the system are broken, or dynamic equilibrium exchange is more frequent, the  $\pi$ - $\pi$  aggregation of the PDI-C6 dye is broken, stretching the intermolecular arrangement, giving the solution a final bright yellow color.

### 2.4. 3D printing, and anti-counterfeiting applications

Given the excellent properties of these supramolecular controlled white light-emitting systems, and that the commercialization of LED technology has promoted research into the application of white light, more and more researchers have sought to incorporate a variety of dyes into supramolecular systems to develop white light applications. A series of dyes with dual fluorescence emission has been obtained in such supramolecular systems due to their two simultaneously generated excited states. Excitation at the appropriate wavelength allows the emission of a single excited state to be balanced, and thus, pure white light emission is produced. Therefore, the preparation of supramolecular systems with white light emission is of great practical importance. For practical applications, the use of Epoxy resin (EP), which has a good film-forming

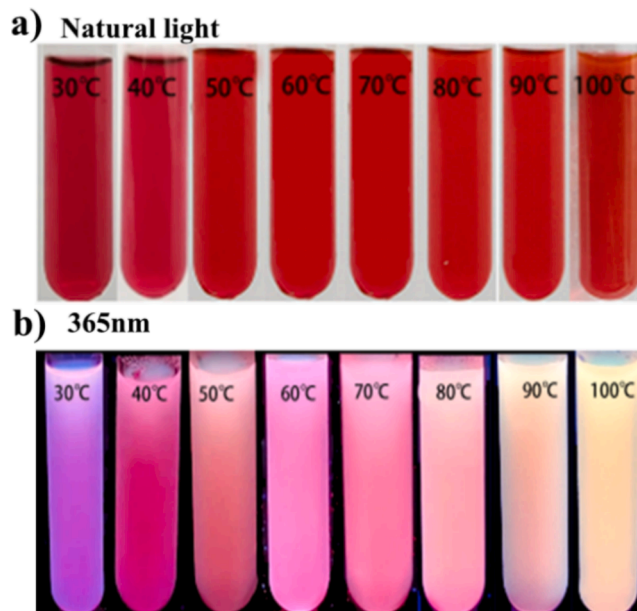
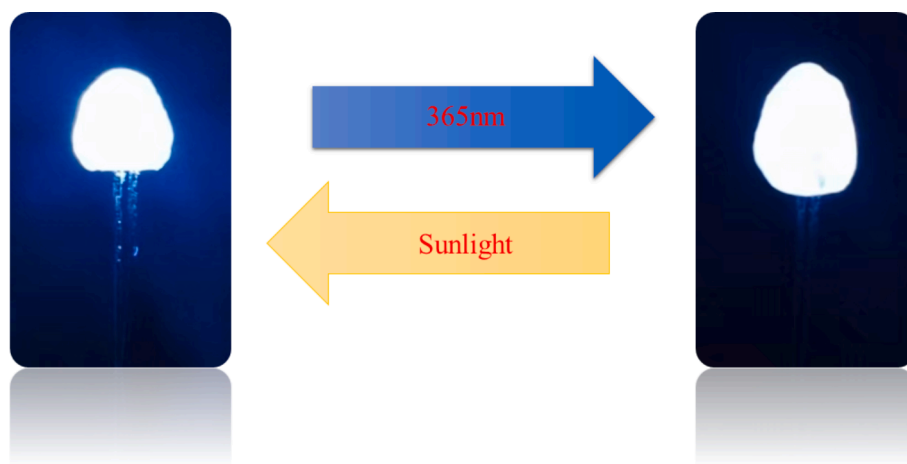


Fig. 7. Fluorescence color changes of the mixed solutions. Fluorescence changes of PDI-C6 (1 mmol), Q[8] (0.1 mmol), and 7-hydroxycoumarin (5 mmol) were observed under natural light (a) and 365 nm UV lamp (b), respectively, with temperature changes (30 °C-100 °C).



**Fig. 8.** The EP film containing PDI-C6@Q[8]@QSD was coated on the UV-LED lamp (the LED lamp with an excitation wavelength of 365 nm was selected), and the white luminescence was shown under sunlight irradiation (left) and 365 nm UV lamp irradiation (right) after power on, respectively.

ability, as a medium for encapsulating supramolecular systems is a preferred method. Additionally, epoxy resins with good film forming ability can be used to encapsulate these dye media. We then conducted the following experiments. Initially, we prepared a special EP film by pouring a solution of PDI-C6 (50  $\mu\text{M}$ ), Q[8] (100  $\mu\text{M}$ ), and quinine sulfate (12.5  $\mu\text{M}$ ) into EP, and then coated this special EP film onto a UV-emitting LED lamp (as shown in Fig. 8). By excitation at 365 nm from this LED lamp, white light emission of 365 nm and visible light can be successfully achieved on the LED lamp, and it was found that under the energized conditions, the LED lamp exhibited white light under UV-365 nm irradiation. In addition, since EP can be used as a good 3D printing material, A and B have the potential to be used as additives in 3D printing materials for the manufacture of white light emission for certain applications. The 3D printer successfully printed roses under UV light using the polymer EP with and without the PDI-C6@Q[8]@Quinine Sulfate additive. Notably, the 3D printing process and the quality of the roses were completely unaffected by the PDI-C6@Q[8]@Quinine Sulfate additive. The roses without the additive were completely transparent in daylight, while the roses with the additive appeared pink in daylight. In the absence of PDI-C6@Q[8]@Quinine Sulfate, the roses exhibited weak blue light emission under 365 nm UV light (as shown in Fig. 9a). Fortunately, roses containing PDI-C6@Q[8]@Quinine Sulfate

exhibited different colors under 365 nm UV light, when printed at 0–4 h with high water content; 3D printed roses exhibit white light under 365 nm UV lamps. After leaving the 3D-printed roses for 4–12 h, the moisture content gradually decreases, and they gradually appear light pink under the ultraviolet lamp, until the water completely evaporates, it shows a bright pink (as shown in Fig. 9b, c, d). whilst there was no significant difference under daylight. In the absence of PDI-C6@Q[8]@Quinine Sulfate, the roses exhibited weak blue emission under 365 nm UV light (as shown in Fig. 9a). there is no obvious difference under daylight. Based on such excellent fluorescence properties, the system can be used to manufacture certain objects with 3D white light emission, thereby illustrating the potential for the application of this white light hybrid system of PDI-C6 in 3D printing. Due to the intrinsic hydrophobic effect of organic chromophores, the multiple mixing of luminescence in the A and B supramolecular systems by varying the content of PDI-C6 and quinine sulfate endows the prepared white light material with optically tunable and reversible properties, which provides a new method and strategy for the practical application of new LED light-emitting devices.

In addition to this, since system B appears as a red solution under natural light and a white light under 365 nm excitation, we applied the white light system to the printing plate in proportion as shown in Fig. 10.

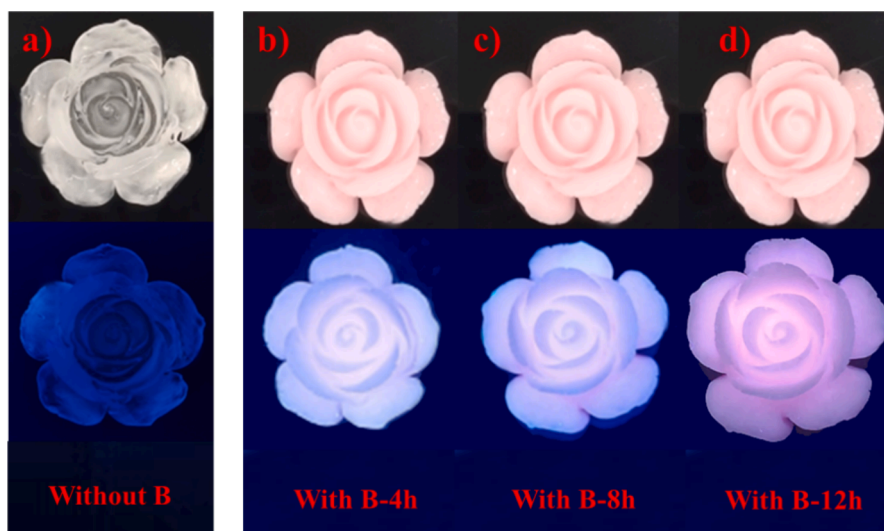


**Fig. 9.** 3D printed roses without (left) and with (right) PDI-C6@Q[8]@QSD, where a indicates roses without PDI-C6@Q[8]@QSD, photographed under daylight (top) and 365 nm (bottom) UV-LED light, and b, c, and d indicate roses with PDI-C6@Q[8]@QSD at 4, 8, and 12 h, photographed under daylight (top) and 365 nm (bottom) UV-LED light.



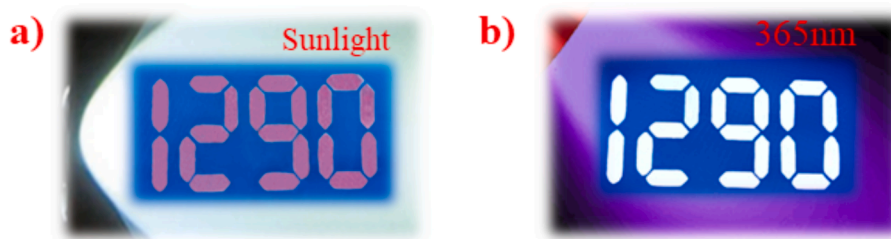


**Fig. 10.** The luminescent pattern of the numeral “1290” based on the repeated application of a solution containing PDI-C6(50  $\mu\text{M}$ ), Q[8] (100  $\mu\text{M}$ ), QSD (12.5  $\mu\text{M}$ ) mixture on the printing plate. Photographed under natural light and 365 nm UV light irradiation, respectively.

The prepared solution of PDI-C6 (0.38 mmol), Q[8] (0.75 mmol), and quinine sulfate (1.5 mmol) was repeatedly applied to the printing plate, and the red number “1290” was displayed under natural light, and the number “1290” was shown in white under 365 nm UV light. Thus, both the application and potential of PDI-C6@Q[8]@Quinine sulfate in anti-counterfeiting materials were demonstrated.

### 3. Conclusion

In summary, we have developed two novel dual-mode orthogonal tunable fluorescence systems using a supramolecular host-guest approach. In system A, 0.2 equal amount of Q[8] is added to A guest molecular solution of PDI-C6@7-hydroxycoumarin (the ratio of two guests is 1:1), or 0.2 equal amount of PDI-C6 is added to A solution of 1.0 equal amount of 7-hydroxycoumarin and 0.1 equiv. of Q[8] (where 7-hydroxycoumarin and Q[8] do not interact) to a solution of the guest molecule and produces blue, yellow, and white fluorescence under a 365 nm UV lamp at 25 °C. The ability to tune and reverse the physical properties is possible in these systems. In addition, system A regulates the host-guest interactions at different temperatures in proportion to trigger a proportional fluorescence response between blue and yellow emissions. The development of supramolecular systems with two-component fluorescent molecules provides a reliable design approach for more complex multi-component fluorescent molecular systems, a strategy that could lead to more orthogonal-controlled fluorescence systems and organic luminescent devices. In the case of system B, when 0.4, 0.5 equiv. of quinine sulfate (where quinine sulfate and Q[8] interact) are added to the PDI-C6 (10  $\mu\text{M}$ ) @ Q[8] (20  $\mu\text{M}$ ) molecular solution, such supramolecular systems facilitate the preparation of stimulated fluorescent materials with white luminescence capabilities because they have excellent luminescence properties. Based on these supramolecular systems, we established a luminescence system consisting of PDI-C6@Q[8]@quinine sulfate. Among the emission capabilities, the system driven by  $\pi$ - $\pi$  stacking shows tunable emission under external stimulation. Flexible operation and good processability can be established using polymeric substrates such as EP to encapsulate the PDI-C6@Q[8]@quinine sulfate-based supramolecular systems to build white light emitters. This strategy may lead to more orthogonally controlled fluorescent systems and organic light-emitting devices for practical applications, such as 365 nm excitation white LED lamps, 3D printing of white light shades, and applications of anti-counterfeit materials. Thus, supramolecular-controlled luminescent systems are not limited to white light-emitting applications, but can also be explored for more multifunctional material applications, which will ignite the enthusiasm of researchers to develop more advanced multifunctional supramolecular materials for various high-tech applications.

### CRedit authorship contribution statement

**Ting Ting Zhang:** Conceptualization, Data curation, Investigation, Project administration. **Xi Nan Yang:** Validation, Formal analysis, Visualization. **Jian Hang Hu:** Data curation, Formal analysis, Software. **Yang Luo:** Formal analysis, Investigation, Validation. **Hou Jing Liu:**

Resources, Supervision, Visualization. **Zhu Tao:** Methodology, Resources. **Xin Xiao:** Funding acquisition, Writing – review & editing. **Carl Redshaw:** Methodology, Supervision, Writing – original draft.

### Declaration of Competing Interest

The authors declare that they have no known competing financial interests or personal relationships that could have appeared to influence the work reported in this paper.

### Data availability

Data will be made available on request.

### Acknowledgments

This work was supported by the National Natural Science Foundation of China (No. 21861011), the Innovation Program for High-level Talents of Guizhou Province (No. 2016-5657), and the Science and Technology Fund of Guizhou Province (No. 2018-5781). CR thanks the EPSRC for an Overseas Travel Grant (EP/R023816/1).

### Appendix A. Supplementary data

Supplementary data to this article can be found online at <https://doi.org/10.1016/j.cej.2022.138960>.

### References

- [1] D. Yang, M. Liu, X. Xiao, Z. Tao, C. Redshaw, Polymeric self-assembled cucurbit[*n*]urils: synthesis, structures, and applications, *Coord. Chem. Rev.* 434 (2021) 213733.
- [2] X.L. Ni, X.S. Chen, Y. Yang, Z. Tao, Facile cucurbit[8]uril-based supramolecular approach to fabricate tunable luminescent materials in aqueous solution, *J. Amer. Chem. Soc.* 138 (2016) 6177–6183.
- [3] A.L. Koner, W.M. Nau, Cucurbituril encapsulation of fluorescent dyes, *Supramol. Chem.* 19 (2007) 55–66.
- [4] B. Kumari, M. Paramasivam, A. Dutta, S. Kanvah, Emission and color tuning of cyanostilbenes and white light emission, *ACS Omega* 3 (2018) 17376–17385.
- [5] Y. Liu, Q. Zhang, W.-H. Jin, T.-Y. Xu, D.-H. Qu, H. Tian, Bistable [2]rotaxane encoding an orthogonally tunable fluorescent molecular system including white-light emission, *Chem. Commun.* 54 (2018) 10642–10645.
- [6] H. Wu, J. Zhao, X.N. Yang, D. Yang, L.X. Chen, C. Redshaw, L.G. Yang, Z. Tao, X. Xiao, A cucurbit[8]uril-based probe for the detection of the pesticide tricyclazole, *Dyes, and Pigments* 199 (2022), 110076.
- [7] F. Biedermann, E. Elmalem, I. Ghosh, W.M. Nau, O.A. Scherman, Strongly fluorescent, switchable perylene bis(diimide) host-guest complexes with cucurbit[8]uril in water, *Angew. Chemie, Int. Ed.* 51 (31) (2012) 7739–7743.
- [8] Y. Jiao, K. Liu, G. Wang, Y. Wang, X. Zhang, Supramolecular free radicals: near-infrared organic materials with enhanced photothermal conversion, *Chem. Sci.* 6 (2015) 3975–3980.
- [9] G.H. Aryal, K. Lu, G. Chen, K.W. Hunter, L. Huang, A colorimetric and fluorescent dual-modal displacement probe based on host-assisted modulation of intramolecular charge transfer and deaggregation, *Chem Commun.* 55 (2019) 13912–13915.
- [10] H. Wang, K.-F. Xue, Y. Yang, H. Hu, J.-F. Xu, X. Zhang, In situ hypoxia-induced supramolecular perylene diimide radical anions in tumors for photothermal therapy with improved specificity, *J. Am. Chem. Soc.* 144 (2022) 2360–2367.

- [11] Y. Yang, Z. An, Visible light induced aqueous RAFT polymerization using a supramolecular perylene diimide/cucurbit[7]uril complex, *Polym. Chem.* 10 (2019) 2801–2811.
- [12] Q. Wang, Q. Zhang, Q.-W. Zhang, X. Li, C.-X. Zhao, T.-Y. Xu, D.-H. Qu, H. Tian, Color-tunable single-fluorophore supramolecular system with assembly-encoded emission, *Nat. Commun.* 11 (2020) 158.
- [13] S. Yang, C.-X. Zhao, S. Crespi, X. Li, Q. Zhang, Z.-Y. Zhang, J. Mei, H. Tian, D.-H. Qu, Reversibly modulating a conformation-adaptive fluorophore in [2]catenane, *Chem.* 7 (2021) 1544–1556.
- [14] C. Chang, H. Tsai, K. Chen, Green perylene bisimide dyes: synthesis, photophysical and electrochemical properties, *Materials* 7 (2014) 5488–5506.
- [15] S. Dou, Y. Wang, X. Zhang, Amphiphilic fluorescence resonance energy-transfer dyes: synthesis, fluorescence, and aggregation behavior in water, *Chem. Eur. J.* 26 (2020) 11503–11510.
- [16] W. Zhang, Y. Luo, J. Zhao, W.-H. Lin, X.-L. Ni, Z. Tao, X. Xiao, C.-D. Xiao, rQ[14]-based AIE Supramolecular Network Polymers as Potential Bioimaging Agents for the Detection of Fe<sup>3+</sup> in Live HeLa Cells, *Sens. Actuators B Chem.* 354 (2022), 131189.
- [17] Q.-Y. Yang, J.-M. Lehn, Bright white-light emission from a single organic compound in the solid state, *Angew. Chem. Int. Ed.* 126 (2014) 4660–4665.
- [18] Y. Luo, S. Gan, W. Zhang, M. Jia, L. Chen, C. Redshaw, Z. Tao, X. Xiao, A new cucurbit[10]uril-based AIE fluorescent supramolecular polymer for cellular imaging, *Mat. Chem. Front.* 6 (8) (2022) 1021–1025.
- [19] H. Li, X. Li, Z.-Q. Cao, D.-H. Qu, H. Agren, H. Tien, A switchable bis-branched [1]rotaxane featuring dual-mode molecular motions and tunable molecular aggregation, *ACS Appl. Mater. Inter.* 6 (2014) 18921–18929.
- [20] W.T. Xu, Y. Luo, W.W. Zhao, M. Liu, G.Y. Luo, Y. Fan, R.L. Lin, Z. Tao, X. Xiao, J. X. Liu, Detecting pesticide dodine by displacement of fluorescent acridine from cucurbit[10]uril macrocycle, *J. Agric. Food Chem.* 69 (2021) 584–591.
- [21] M.H. Lee, N. Park, C. Yi, J.H. Han, J.H. Hong, K.P. Kim, D.H. Kang, J.L. Sessler, C. Kang, J.S. Kim, Mitochondria-immobilized pH-sensitive off-on fluorescent probe, *J. Am. Chem. Soc.* 136 (2014) 14136–14142.
- [22] M. Liu, L. Chen, P. Shan, C. Lian, Z. Zhang, Y. Zhang, Z. Tao, X. Xiao, Pyridine detection using supramolecular organic frameworks incorporating cucurbit[10]uril, *ACS Appl. Mater. Inter.* 13 (2021) 7434–7442.
- [23] Z. Qin, S. Zhao, X. Fang, B. Zhao, J. Deng, K. Pan, Flexible, ultra-Light, and 3D designed white-light-emitting nanofiber aerogel, *Adv. Funct. Mater.* 32 (2022) 2109240.
- [24] W.-T. Xu, Y. Luo, W.-W. Zhao, M. Liu, G.-Y. Luo, Y. Fan, R.-L. Lin, Z. Tao, X. Xiao, J.-X. Liu, Detecting pesticide dodine by displacement of fluorescent acridine from cucurbit[10]uril macrocycle, *J. Agric. Food Chem.* 69 (1) (2021) 584–591.
- [25] R.H. Gao, L.X. Chen, K. Chen, Z. Tao, X. Xiao, Development of hydroxylated cucurbit[n]urils, their derivatives and potential applications, *Coord. Chem. Rev.* 348 (2017) 1–24.
- [26] X. Zhang, S. Rehm, M.M. Safont-Sempere, F. Würthner, Vesicular perylene dye nanocapsules as supramolecular fluorescent pH sensor systems, *Nat. Chem.* 1 (8) (2009) 623–629.
- [27] H. Wu, Y. Zhao, Colour-tunable ultra-long emission, *Nat. Photonics* 13 (6) (2019) 373–375.
- [28] Y. Luo, W. Zhang, M. Liu, J. Zhao, Y. Fan, B. Bian, Z. Tao, X. Xiao, A supramolecular fluorescent probe based on cucurbit[10]uril for sensing the pesticide dodine, *Chinese Chem. Lett.* 32 (1) (2021) 367–370.
- [29] M. Liu, M. Yang, Y. Yao, Y. Zhang, Y. Zhang, Z. Tao, Q. Zhu, G. Wei, B. Bian, X. Xiao, Specific recognition of formaldehyde by a cucurbit[10]uril-based porous supramolecular assembly incorporating adsorbed 1,8-diaminonaphthalene, *J. Mater. Chem. C* 7 (6) (2019) 1597–1603.
- [30] G. Wang, H. Yu, L. Yang, Z. He, L. Zhou, J. Sun, X. Gu, W. Yang, B.Z. Tang, Core-shell fluorescent polymeric particles with tunable white light emission based on aggregation microenvironment manipulation, *Angew. Chemie Int. Ed.* 69 (2021) 25246–25251.
- [31] X.-L. Ni, X. Xiao, H. Cong, L.-L. Liang, K. Cheng, X.-J. Cheng, N.-N. Ji, Q.-J. Zhu, S.-f. Xue, Cucurbit[n]uril-based coordination chemistry: from simple coordination complexes to novel poly-dimensional coordination polymers, *Chem. Soc. Rev.* 42 (2013) 9480–9508.
- [32] W. Zhang, Y. Luo, J. Zhao, W.-H. Lin, X.-L. Ni, Z. Tao, X. Xiao, C.-D. Xiao, rQ[14]-based AIE supramolecular network polymers as potential bioimaging agents for the detection of Fe<sup>3+</sup> in live HeLa cells, *Sens. Actuators B:Chem.* 354 (2022), 131189.
- [33] W. Zhang, Y. Luo, Two-step, sequential, efficient, artificial light-harvesting systems based on twisted cucurbit[14]uril for manufacturing white light emission materials, *Chem. Eng. J.* 446 (2022) 136954.
- [34] W.-H. Jin, H.-H. Lu, Q. Zhang, D.-H. Qu, A dual-mode orthogonally tunable fluorescent system covering the whole white light region, *Mater. Chem. Front.* 4 (2020) 532–536.
- [35] Q. Wang, Q. Zhang, Q.W. Zhang, et al., Color-tunable single-fluorophore supramolecular system with assembly-encoded emission, *Nat. Commun.* 11 (2020) 158.
- [36] F. Tian, D. Jiao, F. Biedermann, O.A. Scherman, Orthogonal switching of a single supramolecular complex, *Nat. Commun.* 3 (2012) 1207.
- [37] M. Zhang, S. Yin, J. Zhang, Z. Zhou, M.L. Saha, C. Lu, P.J. Stang, Metallacycle-colored supramolecular assemblies with tunable fluorescence including white-light emission, *Proc. Natl. Acad. Sci.* 114 (12) (2017) 3044–3049.
- [38] Y.H. Ko, E. Kim, I. Hwang, K. Kim, Supramolecular assemblies built with host-stabilized charge-transfer interactions, *Chem. Commun.* (13) (2007) 1305–1315.
- [39] T.-C. Lee, E. Kalenius, A.I. Lazar, K.I. Assaf, N. Kuhnert, C.H. Grin, J. Jänis, O. A. Scherman, W.M. Nau, Chemistry inside molecular containers in the gas phase, *Nat. Chem.* 5 (2013) 376–382.
- [40] Z. Zong, Q. Zhang, S.-H. Qiu, Q. Wang, C. Zhao, C.-X. Zhao, H. Tian, D.-H. Qu, Dynamic timing control over multicolor molecular emission by temporal chemical locking, *Angew. Chemie. Int. Ed.* 61 (2022) e202116414.
- [41] S. Qiu, Z. Zhang, Y. Wu, F. Tong, K. Chen, G. Liu, L. Zhang, Z. Wang, D.-H. Qu, H. Tian, Vibratile dihydrophenazines with controllable luminescence enabled by precise regulation of  $\pi$ -conjugated wings, *CCS Chem.* 3 (2021) 2239–2248.
- [42] C.R. Li, H.M. Feng, J.Y. Zhao, Z. Li, B. Bian, T.-H. Meng, X.-Y. Hu, H. Wang, X. Xiao, supramolecular interaction between cucurbit[8]uril and the quinolone antibiotic ofloxacin, *Aust. J. Chem.* 72 (2019) 983–989.
- [43] J. Zhang, R.J. Coulston, S.T. Jones, J. Geng, O.A. Scherman, C. Abell, One-Step fabrication of supramolecular microcapsules from microfluidic droplets, *Science* 335 (2012) 690–694.
- [44] J.L. Segura, H. Herrera, P. Bäuerle, Oligothiophene-functionalized naphthalimides and perylene imides: design, synthesis and applications, *J. Mat. Chem.* 22 (2012) 8717–8733.
- [45] J. Yang, H. Miao, Y. Wei, W. Li, Y. Zhu,  $\pi$ - $\pi$  Interaction between self-assembled perylene diimide and 3D graphene for excellent visible-light photocatalytic activity, *Appl. Catal. B.* 240 (2019) 225–233.
- [46] Z. Huang, L. Yang, Y. Liu, Z. Wang, O.A. Scherman, X. Zhang, Supramolecular polymerization promoted and controlled through self-sorting, *Angew. Chem., Int. Ed.* 53 (2014) 5351–5355.
- [47] D. Li, J. Wang, X. Ma, White-light-emitting materials constructed from supramolecular approaches, *Adv. Opt. Mater.* 6 (2018) 1800273.
- [48] X.Y. Zhu, X.N. Yang, H. Wu, Z. Tao, X. Xiao, Construction of supramolecular fluorescent probe by a water-soluble pillar[5]arene and its recognition of carbonate ion, *Bull. Chem. Soc. Jpn* 95 (2022) 116–120.
- [49] J. Wang, X. Gu, H. Ma, Q. Peng, X. Huang, X. Zheng, S.H.P. Sung, G. Shan, J.W. Y. Lam, Z. Shuai, B.Z. Tang, A facile strategy for realizing room temperature phosphorescence and single molecule white light emission, *Nat. Commun.* 9 (2018) 2963.
- [50] H. Feng, Y. Luo, M. Liu, Q. Chen, Z. Tao, X. Xiao, A facile cucurbit[8]uril-based porous assembly: Utilisation in the adsorption of drugs and their controlled release, *New J. Chem.* 45 (2021) 22133–22140.
- [51] Q. Wang, K. Zhang, R.-L. Lin, W.-Q. Sun, M.-F. Ye, X. Xiao, J.-X. Liu, A light-responsive molecular switch based on cucurbit[7]uril and 1,1'-bis(benzyl)-4-[2-(4-pyridyl)-vinyl]-pyridinium dibromide displaying white light emission, *Org. Biomol. Chem.* 20 (6) (2022) 1253–1259.
- [52] K. Yang, G. Yu, Z. Yang, L. Yue, X. Zhang, C. Sun, J. Wei, L. Rao, X. Chen, R. Wang, Supramolecular polymerization-induced nanoassemblies for self-augmented cascade chemotherapy and chemodynamic therapy of tumor, *Angew. Chemie Int. Ed.* 60 (32) (2021) 17570–17578.
- [53] H. Ding, J. Li, G. Xie, G. Lin, R. Chen, Z. Peng, C. Yang, B. Wang, J. Sun, C. Wang, An AIEgen-based 3D covalent organic framework for white light-emitting diodes, *Nat. Commun.* 9 (2018) 5234.
- [54] S. Guo, Q. Huang, Y. Chen, J. Wei, J. Zheng, L. Wang, R. Wang, Synthesis and bioactivity of guanidinium-functionalized Pillar[5]arene as a biofilm disruptor, *Angew. Chemie Int. Ed.* 60 (2020) 618–623.